AIMS Mathematics, 10(10): 22791–22816.
DOI: 10.3934/math.20251013
Received: 19 July 2025
Revised: 17 September 2025
Accepted: 24 September 2025
Published: 09 October 2025

https://www.aimspress.com/journal/Math

Research article

Backstepping-sliding-mode-based prescribed-time control for a class of nonlinear systems with disturbances

Litong Zhou[1], Lichao Feng[1,2,3,*], Nan Ji[2] and Ruicheng Zhang[1]

[1] College of Electrical Engineering, North China University of Science and Technology, Tangshan 063210, China
[2] College of Science, North China University of Science and Technology, Tangshan 063210, China
[3] Hebei Key Laboratory of Data Science and Application, North China University of Science and Technology, Tangshan 063210, China

*** Correspondence:** Email: fenglichao@ncst.edu.cn.

Abstract: This article addresses the prescribed-time stability (PTS) problem for a class of nonlinear strict-feedback systems subject to unknown disturbances. Herein, a novel backstepping-sliding-mode (BSM) composite control structure is proposed: a dynamic time-varying sliding-mode surface is integrated into the final step of the backstepping design, effectively suppressing matched disturbances and simplifying the implementation complexity. Specifically speaking, 1) for systems with known nonlinear terms, time-varying gains are directly embedded within the backstepping virtual control laws to achieve PTS; 2) for the case of unknown nonlinear terms, by combining adaptive laws with the BSM framework, the controlled system is guaranteed to converge within the prescribed-time and maintain globally stability thereafter. Moreover, the prescribed time T_p is designer-prespecified and does not depend on initial conditions or controller gains. Finally, two numerical simulation examples validate the convergence performance and robustness of the proposed approaches.

Keywords: nonlinear strict-feedback systems; sliding-mode control; backstepping method; adaptive control; prescribed-time control
Mathematics Subject Classification: 93C10, 93D05

1. Introduction

Nonlinear dynamics are prevalently applied in various fields such as aerospace, electromechanics, and chemical engineering, and the stability remains a core challenge [1]. Convergence speed and steady-state accuracy are critical indexes for control performance evaluation [2]. Traditionally asymptotic stability ensures systems gradually converge, but typically requires infinite time, rendering them unsuitable for practical applications with rapid responses [3–5]. Subsequently, a finite-time control strategy has been proposed to enable precise convergence within finite time, whose convergence time depends on initial states and tunable parameters [6–8]. Further, fixed-time control emerged to feature convergence time dependent solely on design parameters, independent of initial conditions [9,10]. Yet, the above issues still restricted convergence time to parameter-defined intervals [11,12].

To address the above limitations, prescribed-time stability (PTS) control drives the system state to the equilibrium exactly at any designer-specified time, regardless of initial conditions and controller parameters [13]. This approach of [13] garnered extensive attention, and was applied in linear systems, strict-feedback systems, and temporal control of PDE systems [14–16]. Nevertheless, many existing studies (e.g., [17,18]) focused on reaching PTS within the prescribed time and rarely addressed how to maintain stability after the prescribed time, which demonstrated a drawback for mission-critical scenarios such as missile interception or spacecraft docking with post-convergence robustness [19].

Many recent studies on prescribed-time stability (PTS) have focused on uncertain nonlinear systems [19,20], achieving exact convergence at a designer-specified time and remaining stable thereafter, yet typically under disturbance-free assumptions. Given that robust sliding-mode control (SMC) excels at rejecting external perturbations [21–23], SMC was embedded into the PTS framework to secure prescribed-time convergence for disturbed nonlinear systems [24]; however, the design in [24] presupposed accurately known dynamics and therefore handled parametric uncertainties poorly. In addition, backstepping-sliding-mode (BSM) designs for systems were widely reported [25,26], integral backstepping with integral/terminal (including fractional-order) sliding surfaces further achieved fast or finite-time performance [27], and backstepping was also validated on self-balancing two-wheeled EVs [28]. Furthermore, in the BSM literature, adaptive backstepping was fused with second-order SMC to obtain asymptotic stability for uncertain nonlinear systems [29–30]. Nonetheless, second-order sliding surfaces increase computational burden and require higher-order derivatives, complicating real-time implementation. Moreover, existing BSM schemes (e.g., [25–27,29–30]) remain confined to asymptotically or finite-time guarantees rather than prescribed-time control, leaving the settling time dependent on initial conditions and controller gains. However, PTS is known to enable the designer to preassign a desired convergence time in advance. These observations motivate three open questions: 1) How can we realize PTS for disturbed deterministic or uncertain nonlinear systems while safeguarding post-convergence stability? 2) Can the BSM method be upgraded to meet the stricter PTS requirement? 3) Can a computationally expensive two-order sliding surface be replaced by a cheap method, such as a first-order sliding sufrace, to simultaneously reduce complexity and preserve PTS in the presence of disturbances?

Motivated by these insights, this paper proposes a novel prescribed-time robust controller for nonlinear strict-feedback systems, integrating the backstepping approach with sliding-mode control

to ensure precise prescribed-time convergence and sustained stability thereafter. The key contributions of this work are summarized as follows:

(1) Unlike existing BSM composite frameworks, which have not effectively addressed the PTS problem and often fail to remain stable after the prescribed time under external disturbances, the proposed method achieves precise convergence within the prescribed time and guarantees global stability in the presence of bounded disturbances.

(2) We are the first to realize a prescribed-time BSM scheme by embedding a designer-parameterized, time-varying, first-order sliding surface at the terminal recursion. This makes the prescribed time an explicit design knob and comes with well-posedness and post-prescribed-time robustness guarantees.

(3) In contrast to most existing approaches that rely on second-order sliding-mode control, this work only introduces a time-varying sliding-mode surface with a first-order sliding-mode framework for strict-feedback systems, which simplifies the controller structure, reduces implementation complexity, and preserves strong robustness against matched disturbances.

2. Preliminaries

Consider the following nonlinear strict-feedback system:

$$\begin{cases}\dot{\zeta}_i(t) = \zeta_{i+1}(t) + f_i(\bar{\zeta}_i), i = 1,2\ldots,n-1,\\ \dot{\zeta}_n(t) = v(t) + f_n(\bar{\zeta}_n) + d(t),\end{cases} \tag{1}$$

where $\zeta_i(t) \in R$ is the system state, $\bar{\zeta}_i = [\zeta_1, \zeta_2, \ldots, \zeta_i]^T \in R^i$, $\zeta(t) = \bar{\zeta}_n$, $v(t)$ is the control input, $f_i(\cdot): R^i \to R$ is locally Lipschitz with $f_i(0) = 0$, $i = 1,\ldots,n$, and $d(t)$ represents external disturbances.

For system (1), we aim to propose a prescribed-time controller based on a BSM approach to ensure that the system precisely converges to equilibrium within the prescribed-time T_p and maintains stability thereafter.

Remark 1. Prescribed-time (or predefined-time) stability builds directly on the framework of fixed-time stability (FxTS). The first formal FxTS definition and constructive feedback designs with a uniform settling-time bound independent of the initial conditions were given by Polyakov [9], and later extended using bi-limit and homogeneous Lyapunov tools [31,32]. These results motivated generalizations where the designer assigns an a priori upper bound T_c for the settling time with explicit constructions [33]. More recent work provides Lyapunov-like characterizations and time-scaling methods that generate broad classes of FxT systems with a predefined (often least) upper bound, unifying autonomous/non-autonomous cases [34–36]. Our analysis follows this lineage: we adopt the prescribed-time notion (weak version, $T(x_0) \le T_p$) and show how it can be realized within a backstepping-sliding-mode framework under disturbances.

Remark 2. System (1) belongs to the classical block-controllable canonical (regular) form: the state is partitioned into blocks and used sequentially as quasi-inputs so that the synthesis decomposes into lower-dimensional "elementary" subproblems, where the single-input case reduces to the well-known chain-of-integrators representation. As is known, this block principle, together with motion-separation and hierarchical design, was systematically developed in the foundational literature on block control and regular forms [37–39]. Therefore, the structural reformulation adopted here is standard; our novelty does not lie in the form itself but in upgrading a simple BSM

framework to achieve PTS.

Assumption 1. $d(t)$ is measurable and essentially bounded, i.e., there exists a known $\lambda > 0$ such that $|d(t)| \leq \lambda,\ \forall t \geq 0$.

Definition 1. [20] For given $T_p > 0$, if $\mu(t) > 0, \forall t \in [0, T_p)$, $\mu(t) \to +\infty$ as $t \to T_p^-$, and $\lim_{t \to T_p^-}(T_p - t)\mu(t) = \rho$, where ρ is a positive constant or approaches infinity, then $\mu(t)$ is termed as a prescribed-time adjustment (PTA) function.

Lemma 1. [40] Let $T_p > 0$, $\mu_1(t) = \frac{1}{T_p - t}$, and $V: [0, T_p) \to [0, +\infty)$ is C^1. If there exist constant $k > 0$ and a function $\tilde{d}(t)$ such that

$$\dot{V}(t) \leq -k\mu_1(t)V(t) + \left|\tilde{d}(t)\right|, t \in [0, T_p), \tag{L-1}$$

then $V(t)$ is bounded on $t \in [0, T_p)$ and $\lim_{t \to T_p^-} V(t) = 0$.

Remark 3. In proposition 11 of [40], it is required that

$$\dot{V}(t) \leq -k\tilde{\mu}_1(t)V(t) + \left|\tilde{d}(t)\right|, \tilde{\mu}_1(t) = \frac{T_p}{T_p - t}. \tag{L-2}$$

Hence, our Lemma 1 is another form of Proposition 11 of [40].

3. Main results (controller design)

This section mainly presents the BSM controller to achieve prescribed-time convergence for system (1). The BSM controller is discussed separately for the cases of known $f_i(\cdot)$ and unknown $f_i(\cdot)$.

Define new $\mu(t) = 1/T_p - t$. For simplicity, $\mu(t)$ and $f_i(\cdot)$ will be denoted as μ and f_i. Additionally, we divide the time domain into two stages: $t \in [0, T_p)$ and $t \in [T_p, +\infty)$.

3.1. Prescribed-time control for known f_i

Phase 1 ($0 \leq t < T_p$). In order to simplify the analysis, the following state transitions are performed for system (1):

$$\begin{cases} z_1 = \zeta_1, \\ z_i = \zeta_i - \alpha_{i-1}, i = 2, \ldots, n, \end{cases} \tag{2}$$

where α_{i-1} is the virtual controller and will be designed later. Take

$$Q_{n-1} = \frac{1}{2}\sum_{j=1}^{n-1} z_j^2. \tag{3}$$

In the following, a backstepping approach will be used to construct the prescribed-time controller for Phase 1. It contains n steps as below.

Step 1. According to (1) and (2),

$$\dot{z}_1 = \zeta_2 + f_1 = z_2 + \alpha_1 + f_1. \tag{4}$$

Design

$$\alpha_1 = -c_1\mu z_1 - f_1, \tag{5}$$

where c_1 is a design parameter with $c_1 > n$. Choose $Q_1 = \frac{1}{2}z_1^2$, and from (4) and (5),

$$\dot{Q}_1 = -c_1\mu z_1^2 + z_1 z_2. \tag{6}$$

Step i ($2 \le i \le n-1$). According (1) and (2),

$$\dot{z}_i = \dot{\zeta}_i - \dot{\alpha}_{i-1} = \zeta_{i+1} + f_i - \dot{\alpha}_{i-1} = z_{i+1} + \alpha_i + f_i - \dot{\alpha}_{i-1}. \tag{7}$$

Design

$$\alpha_i = -c_i\mu z_i - f_i + \dot{\alpha}_{i-1} - z_{i-1}, \tag{8}$$

where c_i is a design parameter with $c_i > n - i + 1$. Choose $Q_i = Q_{i-1} + \frac{1}{2}z_i^2$, and from (7) and (8),

$$\dot{Q}_i = \dot{Q}_{i-1} + z_i\dot{z}_i = \dot{Q}_{i-1} + z_i(z_{i+1} + \alpha_i + f_i - \dot{\alpha}_{i-1}) = -\sum_{j=1}^{i} c_j\mu z_j^2 + z_i z_{i+1}. \tag{9}$$

Step n. Similarly,

$$\dot{z}_n = \dot{\zeta}_n - \dot{\alpha}_{n-1} = v + f_n + d(t) - \dot{\alpha}_{n-1}. \tag{10}$$

A new dynamic sliding variable is designed as

$$s = z_n + (T_p - t)z_{n-1} = z_n + \frac{1}{\mu}z_{n-1}, \tag{11}$$

and thus

$$\dot{s} = v + f_n + d(t) - \dot{\alpha}_{n-1} - z_{n-1} + \frac{1}{\mu}\dot{z}_{n-1}. \tag{12}$$

Define

$$Q_n = Q_{n-1} + \frac{1}{2}s^2, \tag{13}$$

and then

$$\dot{Q}_n = \dot{Q}_{n-1} + s\dot{s} = -\sum_{j=1}^{n-1} c_j\mu z_j^2 + z_{n-1}\left(s - \frac{1}{\mu}z_{n-1}\right)$$

$$+ s(v + f_n + d(t) - \dot{\alpha}_{n-1} - z_{n-1} + \frac{1}{\mu}\dot{z}_{n-1}). \tag{14}$$

Next, v is designed as

$$v = -c_n\mu s - f_n + \dot{\alpha}_{n-1} - \frac{1}{\mu}\dot{z}_{n-1} - \lambda sign(s), \tag{15}$$

where c_n is a design parameter with $c_n > 1$. Then, from $sd(t) \le s\lambda sign(s)$,

$$\dot{Q}_n = -\sum_{j=1}^{n-2} c_j \mu z_j^2 - (c_{n-1} + \frac{1}{\mu})\mu z_{n-1}^2 - c_n \mu s^2 \leq -c\mu Q_n, \tag{16}$$

where $c = 2\,min\{c_1, \ldots, c_{n-1} + \frac{1}{\mu}, c_n\}$.

Remark 4. The sliding variable design (11) here is motivated by the fact that the unknown disturbance directly affects the n-th subsystem. Accordingly, the time-varying sliding-mode surface (11) involves only the n-th-order and $(n-1)$-th-order error terms. This design effectively suppresses high-order disturbances and accelerates the convergence of preceding error dynamics. Additionally it simultaneously avoids the structural complexity and computational burden compared with a conventionally global sliding-mode surface.

Phase 2 ($t \geq T_p$). Select the sliding variable $s = z_n + z_{n-1}$, and set up the virtual controller and the controller:

$$\alpha_1 = -c_1 z_1 - f_1, \tag{17}$$

$$\alpha_i = -c_i z_i - f_i + \dot{\alpha}_{i-1} - z_{i-1}, \tag{18}$$

$$v = -c_n s - f_n + \dot{\alpha}_{n-1} - z_{n-1} - \dot{z}_{n-1} - \lambda sign(s). \tag{19}$$

Similarly to (15), obtain

$$\dot{Q}_n \leq 0. \tag{20}$$

Remark 5. After the prescribed time is reached, the PTA gain μ (see Definition 1) is fixed at $\mu = 1$. Simply substituting this constant for the time-varying μ of Phase 1 virtual and actual controllers directly yields the Phase 2 controllers.

Theorem 1. For $T_p > 0$, one can design time-varying prescribed-time controllers (15) on $[0, T_p)$ and (19) on $[T_p, +\infty)$ such that system (1) with known $f_i(\cdot)$ can converge to the equilibrium point at T_p and remain stable thereafter.

Proof. Based on (16), due to Lemma 1, it is easy to obtain $\lim\limits_{t \to T_p^-} Q_n = 0$, which implies $\lim\limits_{t \to T_p^-} z_i = \lim\limits_{t \to T_p^-} s = 0$, $i = 1,2,\ldots,n$. Further, for (4) and (5), we have

$$z_1 = z_1(0)(1 - \frac{t}{T_p})^{c_1} + (T_p - t)^{c_1} \int_0^t \frac{z_2}{(T_p - \sigma)^{c_1}}\, d\sigma. \tag{21}$$

Then dividing it by $(T_p - t)^k$ with $k \leq c_1$, one is able to get

$$\lim_{t \to T_p^-} \frac{z_1}{(T_p - t)^k} = \lim_{t \to T_p^-} \frac{z_2}{(c_1 - k)(T_p - t)^{k-1}}. \tag{22}$$

Then, when $k = 1$,

$$\lim_{t \to T_p^-} \frac{z_1}{(T_p - t)} = 0 \Rightarrow \lim_{t \to T_p^-} \dot{z}_1 = 0 \Rightarrow \lim_{t \to T_p^-} \alpha_1 = 0 \Rightarrow \lim_{t \to T_p^-} \zeta_2 = 0 \Rightarrow \lim_{t \to T_p^-} f_2 = 0. \tag{23}$$

Similarly, we can easily get

$$\lim_{t\to T_p^-}\frac{z_i}{(T_p-t)^{k_1}}=\lim_{t\to T_p^-}\frac{z_{i+1}-z_{i-1}}{(c_i-k_1)(T_p-t)^{k_1-1}}, \tag{24}$$

where k_1 is a design parameter with $k_1<c_i,\ i=2,\ldots,n-1$. Thus,

$$\lim_{t\to T_p^-}\frac{z_2}{T_p-t}=0,\ \lim_{t\to T_p^-}\frac{z_1}{(T_p-t)^2}=0,\ \lim_{t\to T_p^-}\frac{\dot{z}_1}{T_p-t}=0\Rightarrow\lim_{t\to T_p^-}\dot{\alpha}_1=0$$
$$\Rightarrow\lim_{t\to T_p^-}\alpha_2=0\Rightarrow\lim_{t\to T_p^-}\zeta_3=0\Rightarrow\ldots\Rightarrow\lim_{t\to T_p^-}\zeta_n=0,\ \lim_{t\to T_p^-}f_n=0. \tag{25}$$

Similarly to (24), we have $\lim_{t\to T_p^-}\frac{z_n}{(T_p-t)}=0$, and therefore $\lim_{t\to T_p^-}\frac{s}{(T_p-t)}=0$. Then due to (25), it is easy to confirm $\lim_{t\to T_p^-}v$ is bounded. Due to (20), we obtain $Q_n(t)\equiv 0, t\geq T_p$, and then $\zeta_i(t)\equiv 0$, $t\geq T_p$. So it can be seen that the system remains stable even after T_p.

Remark 6. To cope with the discontinuity and the PTA gain that may blow up as $t\to T_p$, trajectories are interpreted as generalized Filippov solutions. On any compact interval not containing T_p, when the closed-loop vector field is single-valued and locally Lipschitz, the classical Carathéodory solution and Filippov solution coincide. At $t=T_p$ we impose a continuous transition: there is no state reset, and the trajectory for $t\geq T_p$ is initialized at the left limit, i.e., $x(T_p)=x(T_p^-)$. Under standard Filippov regularity, such generalized solutions are continuable across T_p (see [41]). This solution framework is adopted by this paper.

Remark 7. Reference [20] elegantly addressed adaptive prescribed-time stabilization for uncertain strict-feedback systems in the disturbance-free case. The stability on $[T_p,+\infty)$ is ensured by setting $v=0$. However, if the strategy of [20] is designed for system (1) here, the PTS on $[T_p,+\infty)$ will not be achieved for the term $d(t)$. Compared with that, our approach here well-ensures the stability under external perturbations on $[T_p,+\infty)$.

Remark 8. Compared with fixed-time controllers [9–11,31–32,42], whose settling-time bound is independent of initial conditions but affected by controller gains, the proposed PTS scheme allows the designer to preassign the convergence time T_p a priori. In contrast to the BSM scheme in [29], which guarantees asymptotic stabilization and mitigates matched disturbances via the sliding layer, the present method achieves prescribed-time regulation. For a continuous implementation by replacing $sign(\cdot)$ by $tanh(\cdot/\varepsilon)$ to avoid discontinuity, the post-T_p state becomes uniformly ultimately bounded with the neighborhood radius being proportional to the boundary-layer width ε, which yields practical prescribed-time stability in the presence of implementation constraints.

3.2. Prescribed-time control for unknown $\boldsymbol{f_i}$

For the case where function $f(\cdot)$ is unknown, the adaptive control approach is adopted. Assume each $\boldsymbol{f_i}$ has the following linearly parameterized form,

$$f_i(\bar{\zeta}_i)=\theta^T\varphi_i(\bar{\zeta}_i), i=1,2,\ldots,n, \tag{26}$$

where $\varphi_i(\cdot):R^i\to R^r$ is known with $\varphi_i(0)=0$, $\theta\in R^r$ represents an unknown constant parameter vector, and we set $\varphi(\cdot)=(\varphi_1,\ldots,\varphi_n)$. Based on this, system (1) is converted into a

parametric-dependent model, and an adaptive law is designed to estimate θ online.

To simplify the analysis, the following state transformation is introduced for uncertain system (1):

$$\begin{cases} w_1 = \zeta_1 \\ w_i = \zeta_i - \beta_{i-1}, i = 2, \ldots, n, \end{cases} \tag{27}$$

where β_{i-1} is the virtual controller. In subsequent steps, we select

$$Q = W_1 + W_2, \ W_1 = \frac{1}{2}\sum_{j=1}^{n-1} w_j^2 + \frac{1}{2}s^2, \ W_2 = \frac{1}{2}\tilde{\theta}^T \Gamma^{-1}\tilde{\theta}, \tag{28}$$

where s is defined in (40) below, $\tilde{\theta} = \theta - \hat{\theta}$, $\hat{\theta}$ is the estimate of θ, and $\Gamma \in R^{r\times r}$ is positive definite. The subsequent prescribed-time controller construction is based on the BSM method.

Phase 1 ($0 \le t < T_p$).

Step 1. According to (1), (26), and (27),

$$\dot{w}_1 = w_2 + \beta_1 + \theta^T \varphi_1. \tag{29}$$

We design

$$\beta_1 = -g_1 \mu w_1 - \hat{\theta}^T \varphi_1, \tag{30}$$

where g_1 is a design parameter with $g_1 > n$. We choose $Q_1 = \frac{1}{2}{w_1}^2 + W_2$, and then

$$\dot{Q}_1 = -g_1 \mu {w_1}^2 + w_1 w_2 + \tilde{\theta}^T(\tau_1 - \Gamma^{-1}\dot{\hat{\theta}}), \tag{31}$$

where $\tau_1 = w_1 \varphi_1$.

Step 2. According to (1), (26), and (27),

$$\dot{w}_2 = w_3 + \beta_2 + \theta^T \varphi_2 - \dot{\beta}_1 \ = w_3 + \beta_2 + \theta^T \varphi_2 - \frac{\partial \beta_1}{\partial \hat{\theta}}\dot{\hat{\theta}} - \frac{\partial \beta_1}{\partial \zeta_1}(\zeta_2 + \theta^T \varphi_1) - \frac{\partial \beta_1}{\partial t}. \tag{32}$$

We design

$$\beta_2 = -g_2 \mu w_2 - w_1 - \hat{\theta}^T \varphi_2 + \frac{\partial \beta_1}{\partial \hat{\theta}}\Gamma \tau_2 + \frac{\partial \beta_1}{\partial \zeta_1}(\zeta_2 + \hat{\theta}^T \varphi_1) + \frac{\partial \beta_1}{\partial t}, \tag{33}$$

where g_2 is a design parameter with $g_2 > n - 1$, $\tau_2 = \tau_1 + w_2(\varphi_2 - \frac{\partial \beta_1}{\partial \hat{\theta}}\varphi_1)$. We choose $Q_2 = Q_1 + \frac{1}{2}w_2^2$, and then

$$\dot{Q}_2 = -\mu \sum_{j=1}^{2} g_j w_j^2 + \tilde{\theta}^T(\tau_2 - \Gamma^{-1}\dot{\hat{\theta}}) + \frac{\partial \beta_1}{\partial \hat{\theta}} w_2(\Gamma \tau_2 - \dot{\hat{\theta}}) + w_2 w_3. \tag{34}$$

Step i ($3 \le i \le n-1$). According to (1), (26), and (27),

$$\dot{w}_i = w_{i+1} + \beta_i + \theta^T \varphi_i - \dot{\beta}_{i-1} \ = w_{i+1} + \beta_i + \theta^T \varphi_i$$

$$-\frac{\partial \beta_{i-1}}{\partial \hat{\theta}}\dot{\hat{\theta}}-\sum_{j=1}^{i-1}\frac{\partial \beta_{i-1}}{\partial \zeta_j}(\zeta_{j+1}+\theta^T\varphi_j)-\frac{\partial \beta_{i-1}}{\partial t}. \tag{35}$$

We esign

$$\beta_i=-g_i\mu w_i-w_{i-1}-\hat{\theta}^T\varphi_i+\frac{\partial \beta_{i-1}}{\partial \hat{\theta}}\Gamma\tau_i+\sum_{j=1}^{i-1}\frac{\partial \beta_{i-1}}{\partial \zeta_j}(\zeta_{j+1}+\hat{\theta}^T\varphi_j)$$
$$+(\varphi_i-\sum_{j=1}^{i-1}\frac{\partial \beta_{i-1}}{\partial \zeta_j}\varphi_j)\,\Gamma\sum_{j=2}^{i-1}\frac{\partial \beta_{j-1}}{\partial \hat{\theta}}w_j+\frac{\partial \beta_{i-1}}{\partial t}, \tag{36}$$

where g_i is a design parameter with $g_i>n-i+1$, $\tau_i=\tau_{i-1}+w_i(\varphi_i-\sum_{j=1}^{i-1}\frac{\partial \beta_{i-1}}{\partial \zeta_j}\varphi_j)$, and we choose $Q_i=Q_{i-1}+\frac{1}{2}w_i^2$. Then

$$\dot{Q}_i=-\mu\sum_{j=1}^{i}g_jw_j^2+\tilde{\theta}^T(\tau_i-\Gamma^{-1}\dot{\hat{\theta}})+\sum_{j=2}^{i}\frac{\partial \beta_{j-1}}{\partial \hat{\theta}}w_j(\Gamma\tau_i-\dot{\hat{\theta}})+w_iw_{i+1}. \tag{37}$$

Step n. Similarly,

$$\dot{w}_n=v+\theta^T\varphi_n+d(t)-\dot{\beta}_{n-1}=v+\theta^T\varphi_n+d(t)$$
$$-\frac{\partial \beta_{n-1}}{\partial \hat{\theta}}\dot{\hat{\theta}}-\sum_{j=1}^{n-1}\frac{\partial \beta_{n-1}}{\partial \zeta_j}(\zeta_{j+1}+\theta^T\varphi_j)-\frac{\partial \beta_{n-1}}{\partial t}. \tag{38}$$

Similarly to (11), we design the dynamic sliding variable

$$s=w_n+(T_p-t)w_{n-1}, \tag{39}$$

and thus

$$\dot{s}=v+\theta^T\varphi_n+d(t)-\dot{\beta}_{n-1}-w_{n-1}+\frac{1}{\mu}\dot{w}_{n-1}. \tag{40}$$

We define

$$Q=Q_n=Q_{n-1}+\frac{1}{2}s^2. \tag{41}$$

Next, we design the adaptive law $\dot{\hat{\theta}}$ and controller v for system (1),

$$\dot{\hat{\theta}}=\Gamma\tau_s-g_m\mu\hat{\theta}, \tag{42}$$

$$v=-g_n\mu s-\hat{\theta}^T\varphi_n-\lambda sign(s)+\frac{\partial \beta_{n-1}}{\partial \hat{\theta}}\dot{\hat{\theta}}+\frac{\partial \beta_{n-1}}{\partial t}$$
$$+\sum_{j=1}^{n-1}\frac{\partial \beta_{n-1}}{\partial \zeta_j}(\zeta_{j+1}+\hat{\theta}^T\varphi_j)-\frac{1}{\mu}(w_n+\beta_{n-1}+\hat{\theta}^T\varphi_{n-1}-\frac{\partial \beta_{n-2}}{\partial \hat{\theta}}\dot{\hat{\theta}}$$
$$-\frac{\partial \beta_{n-2}}{\partial t}-\sum_{j=1}^{n-2}\frac{\partial \beta_{n-2}}{\partial \zeta_j}(\zeta_{j+1}+\hat{\theta}^T\varphi_j))+(\varphi_n-\sum_{j=2}^{n-1}\frac{\partial \beta_{n-1}}{\partial \zeta_j}\varphi_j$$

$$+\frac{1}{\mu}(\varphi_{n-1}-\sum_{j=1}^{n-2}\frac{\partial\beta_{n-2}}{\partial\zeta_j}\varphi_j))\Gamma\sum_{j=2}^{n-1}\frac{\partial\beta_{j-1}}{\partial\hat{\theta}}w_j-\frac{1}{s}g_m\mu\hat{\theta}\sum_{j=2}^{n-1}\frac{\partial\beta_{j-1}}{\partial\hat{\theta}}w_j, \tag{43}$$

where $\tau_s=\tau_{n-1}+s(\varphi_n-\sum_{j=1}^{n-1}\frac{\partial\beta_{n-1}}{\partial\zeta_j}\varphi_j+\frac{1}{\mu}(\varphi_{n-1}-\sum_{j=1}^{n-2}\frac{\partial\beta_{n-2}}{\partial\zeta_j}\varphi_j))$, g_n is a design parameter with $g_n>1$, and g_m is a design parameter with $g_m>0$. Then, from $sd(t)\le s\lambda sign(s)$,

$$\begin{aligned}
\dot{Q}=\dot{Q}_n&=-\sum_{j=1}^{n-2}g_j\mu w_j^2-(g_{n-1}+\tfrac{1}{\mu})\mu w_{n-1}^2-g_n\mu s^2+\tilde{\theta}^T(\tau_s-\Gamma^{-1}\dot{\hat{\theta}})+\sum_{j=2}^{n-1}\frac{\partial\beta_{j-1}}{\partial\hat{\theta}}w_j(\Gamma\tau_s-\dot{\hat{\theta}})\\
&=-\sum_{j=1}^{n-2}g_j\mu w_j^2-(g_{n-1}+\frac{1}{\mu})\mu w_{n-1}^2-g_n\mu s^2+g_m\mu\tilde{\theta}^T\Gamma^{-1}\hat{\theta}\\
&=-\sum_{j=1}^{n-2}g_j\mu w_j^2-(g_{n-1}+\frac{1}{\mu})\mu w_{n-1}^2-g_n\mu s^2+g_m\mu\tilde{\theta}^T\Gamma^{-1}(\theta-\tilde{\theta})\\
&=-\sum_{j=1}^{n-2}g_j\mu w_j^2-(g_{n-1}+\frac{1}{\mu})\mu w_{n-1}^2-g_n\mu s^2-g_m\mu\tilde{\theta}^T\Gamma^{-1}\tilde{\theta}+g_m\mu\tilde{\theta}^T\Gamma^{-1}\theta\\
&\le-\sum_{j=1}^{n-2}g_j\mu w_j^2-(g_{n-1}+\frac{1}{\mu})\mu w_{n-1}^2-g_n\mu s^2-g_m\mu\tilde{\theta}^T\Gamma^{-1}\tilde{\theta}+\frac{1}{2}g_m\mu\tilde{\theta}^T\Gamma^{-1}\tilde{\theta}+\frac{1}{2}g_m\mu\theta^T\Gamma^{-1}\theta\\
&=-\sum_{j=1}^{n-2}g_j\mu w_j^2-(g_{n-1}+\frac{1}{\mu})\mu w_{n-1}^2-g_n\mu s^2-\frac{1}{2}g_m\mu\tilde{\theta}^T\Gamma^{-1}\tilde{\theta}+\frac{1}{2}g_m\mu\theta^T\Gamma^{-1}\theta\\
&=-g\mu Q_n+D,
\end{aligned} \tag{44}$$

where $g=2\,min\{g_1,\dots,g_{n-1}+\frac{1}{\mu},g_n,\frac{1}{2}g_m\}$ and $D=\frac{1}{2}g_m\mu\theta^T\Gamma^{-1}\theta$.

Phase 2 ($t\ge T_p$). As in Section 3.1, we choose the sliding variable $s=w_n+w_{n-1}$, and set up the virtual controller, controller, and adaptive update law,

$$\beta_1=-g_1w_1-\hat{\theta}^T\varphi_1, \tag{45}$$

$$\beta_2=-g_2w_2-w_1-\hat{\theta}^T\varphi_2+\frac{\partial\beta_1}{\partial\hat{\theta}}\Gamma\tau_2+\frac{\partial\beta_1}{\partial\zeta_1}(\zeta_2+\hat{\theta}^T\varphi_1), \tag{46}$$

$$\begin{aligned}
\beta_i=&-g_iw_i-w_{i-1}-\hat{\theta}^T\varphi_i+\frac{\partial\beta_{i-1}}{\partial\hat{\theta}}\Gamma\tau_i+\sum_{j=1}^{i-1}\frac{\partial\beta_{i-1}}{\partial\zeta_j}(\zeta_{j+1}+\hat{\theta}^T\varphi_j)\\
&+(\varphi_i-\sum_{j=1}^{i-1}\frac{\partial\beta_{i-1}}{\partial\zeta_j}\varphi_j)\,\Gamma\sum_{j=2}^{i-1}\frac{\partial\beta_{j-1}}{\partial\hat{\theta}}w_j,
\end{aligned} \tag{47}$$

$$\begin{aligned}
v=&-g_ns-\hat{\theta}^T\varphi_n-\lambda sign(s)+\frac{\partial\beta_{n-1}}{\partial\hat{\theta}}\dot{\hat{\theta}}\\
&+\sum_{j=1}^{n-1}\frac{\partial\beta_{n-1}}{\partial\zeta_j}(\zeta_{j+1}+\hat{\theta}^T\varphi_j)-w_{n-1}-(w_n+\beta_{n-1}
\end{aligned}$$

$$+\hat{\theta}^T\varphi_{n-1}-\frac{\partial\beta_{n-2}}{\partial\hat{\theta}}\dot{\hat{\theta}}-\sum_{j=1}^{n-2}\frac{\partial\beta_{n-2}}{\partial\zeta_j}(\zeta_{j+1}+\hat{\theta}^T\varphi_j)$$

$$+(\varphi_n-\textstyle\sum_{j=1}^{n-1}\frac{\partial\beta_{n-1}}{\partial\zeta_j}\varphi_j+\varphi_{n-1}-\sum_{j=1}^{n-2}\frac{\partial\beta_{n-2}}{\partial\zeta_j}\varphi_j)\,\Gamma\sum_{j=2}^{n-1}\frac{\partial\beta_{j-1}}{\partial\hat{\theta}}w_j, \tag{48}$$

$$\dot{\hat{\theta}}=\Gamma\tau_{s1}, \tag{49}$$

where $\tau_{s1}=\tau_{n-1}+s(\varphi_n-\sum_{j=1}^{n-1}\frac{\partial\beta_{n-1}}{\partial\zeta_j}\varphi_j+\varphi_{n-1}-\sum_{j=1}^{n-2}\frac{\partial\beta_{n-1}}{\partial\zeta_j}\varphi_j)$.

Similarly to (44), we obtain

$$\dot{Q}_n\le -gW_1\le 0. \tag{50}$$

Theorem 2. For $T_p>0$, one can design time-varying prescribed-time controllers (42), (43) on $[0,T_p)$ and (48), (49) on $[T_p,+\infty)$ such that system (1) with unknown $f_i(\cdot)$ can converge to the equilibrium point at T_p and remain stable thereafter.

Proof. Similarly to Theorem 1 and by Lemma 1, we obtain

$$\lim_{t\to T_p^-}Q=\lim_{t\to T_p^-}Q_n=0, \tag{51}$$

so it is easy to get $\lim_{t\to T_p^-}w_i=\lim_{t\to T_p^-}s=\lim_{t\to T_p^-}\tilde{\theta}=0, i=1,2,\ldots,n.$

Similarly to Theorem 1, it is easy to obtain that $\lim_{t\to T_p^-}\beta_i=0, i=1,\ldots,n-1$, $\lim_{t\to T_p^-}\zeta_i=0$, $i=1,\ldots,n$ and $\lim_{t\to T_p^-}\frac{s}{(T_p-t)}=0$. Due to (44), $\lim_{t\to T_p^-}v$ is bounded. Due to (50), we obtain $Q_n(t)\equiv 0$, $t\ge T_p$, and then $\zeta_i(t)\equiv 0, t\ge T_p$. So it can be seen that the system remains stable after T_p.

Remark 9. We adopt the sliding-mode surface in the n-th-order subsystem to deal with $\dot{\beta}_{n-1}$, and adopts the parametric hysteresis design method to deal with the uncertain paramater in $\dot{\beta}_{n-1}$. Finally, only one parameter estimation is needed to solve the control system under the non-matching condition, thus avoiding the over-parameterization problem.

Remark 10. In [28], only backstepping is used to achieve convergence before a prescribed-time with errors accuracy on $[T_p,+\infty)$, but our BSM approach is able to solve this problem on $[T_p,+\infty)$. Moreover, we further extend the uncertainty range of the nonlinear terms in [24,43] so that the proposed method can be adapted to more general and complex nonlinear systems.

Remark 11. Compared with the BSM method in [29,30], which guarantees asymptotic stabilization and finite-time convergence, the proposed method can ensure prescribed-time convergence of the closed-loop states in the ideal case.

Remark 12. This paper enforces prescribed-time regulation using a time-varying gain that grows as the deadline is approached, and our analysis centers on convergence. We do not yet quantify internal signals nor treat sensor noise and actuator limits. Recent studies provided finite-gain redesigns that keep internal signals bounded while preserving a prescribed-time bound, offering uniform Lyapunov stability and noise-accuracy characterizations; see [44,45]. In parallel, fundamental limitations for "hard-deadline" prescribed-time algorithms were established, explaining potential sensitivity to

small noise near the deadline [46]. In future work, we will 1) adopt finite-gain and early-switch PTA profiles inspired by [44,45]; 2) derive uniform bounds on the sliding variable and control effort under measurement noise and actuator saturation; and 3) compare our design with soft-deadline and least-UBST(Upper Bound of the Settling Time) variants in light of [46]. These steps convert the current convergence guarantees into quantified robustness results.

Remark 13. Classical time-varying sliding (time-base generator, TBG) designs shape a moving sliding manifold so that the convergence time is designer-specified; the tracking error enters a small neighborhood by the deadline and typically decays exponentially thereafter [47–49]. In contrast, we use a single first-order, time-varying sliding surface only in the terminal backstepping step to enforce a designer-chosen prescribed time under matched disturbances, without second-order sliding or bounds on the sliding-surface derivative. The TBG/second-order literature is instructive, and we will report a systematic quantitative comparison and explore integration in future work.

4. Simulation results

Example 1. Consider a one-link robot manipulator [50] with the following dynamics:

$$M\ddot{q} + \frac{1}{2}mgl\,sin\,q + \dot{q} = u + d(t), \tag{52}$$

where $q \in R$ and $\dot{q} \in R$ are the angle and velocity, respectively; $M = 1$ denotes the moment of inertia; $g = 9.8\,\mathrm{N/kg}$; $m = 1\,\mathrm{kg}$ and $l = 1\,\mathrm{m}$ denote the mass and the length of the link, respectively; and $d(t)$ denotes the external disturbance. Then the dynamics in (52) can be expressed as

$$\begin{cases} \dot{\zeta}_1(t) = \zeta_2(t) \\ \dot{\zeta}_2(t) = f(\zeta) + v(t) + d(t), \end{cases} \tag{53}$$

where $\zeta_1 = q, \zeta_2 = \dot{q}, f(\zeta) = -\frac{1}{2}mgl\,sin\,\zeta_1 - \zeta_2$, which becomes $\dot{\zeta}_2(t) = f(\zeta) + g(\zeta)v(t) + M^{-1}d(t)$ in [50] for $M = 1$ and $g(\zeta) = 1$. Assume $d(t) = 0.2\,cos(\,0.5t)$.Then $|0.2\,cos(\,0.5t)| \leq \lambda = 0.2$. Take $T_p = 1.5$ (chosen by task requirements) and two initial conditions $(\zeta_1(0), \zeta_2(0)) = (2,-1), (-1,2)$.

Under the strategy of [20], from Figure 1, system (53) cannot be stabilized on $[T_p, +\infty)$. Hence, it is necessary to employ a new strategy, such as our strategy here.

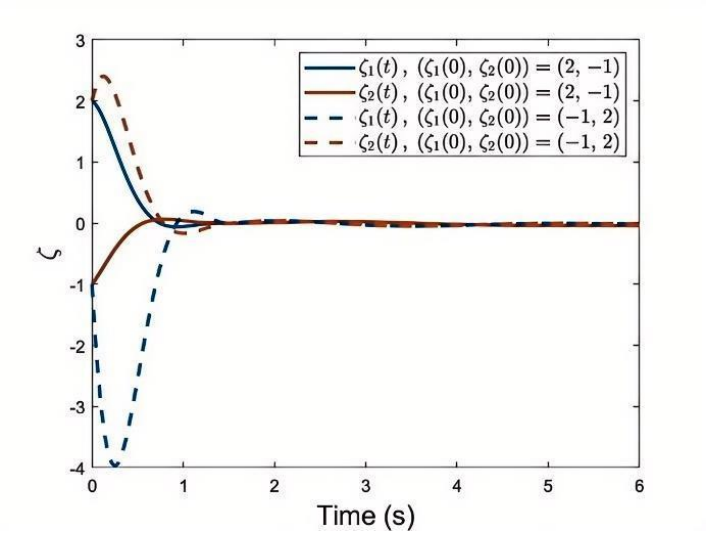

Figure 1. Responses of system (53) under the strategy of [20] with different initial conditions.

According to the above proposed control algorithm, the controller is designed as

$$v(t) = \begin{cases} -c_2\mu(t)s - 4.9\,sin\,\zeta_1 - \zeta_2 - 0.2\,sgn(s) + \dot{\alpha}_1 - \frac{1}{\mu}\dot{z}_1, t \in [0, T_p), \\ -c_2 s - 4.9\,sin\,\zeta_1 - \zeta_2 - 0.2\,sgn(s) + \dot{\alpha}_1 - z_1 - \dot{z}_1, t \in [T_p, +\infty), \end{cases} \tag{54}$$

$$\mu(t) = \begin{cases} \frac{1}{T_p - t}, t \in [0, T_p), \\ 1, t \in [T_p, +\infty), \end{cases} \tag{55}$$

where $\alpha_1 = -c_1\mu z_1$, $\dot{\alpha}_1 = -c_1\dot{\mu}z_1 - c_1\mu\dot{z}_1$, $\dot{z}_1 = \zeta_2$, $s = z_2 + \frac{1}{\mu}z_1, t \in [0,4)$, $s = z_2 + z_1, t \in [4, +\infty)$. Let $c_1 = c_2 = 4$, and the simulation results are shown in Figures 2 to 4.

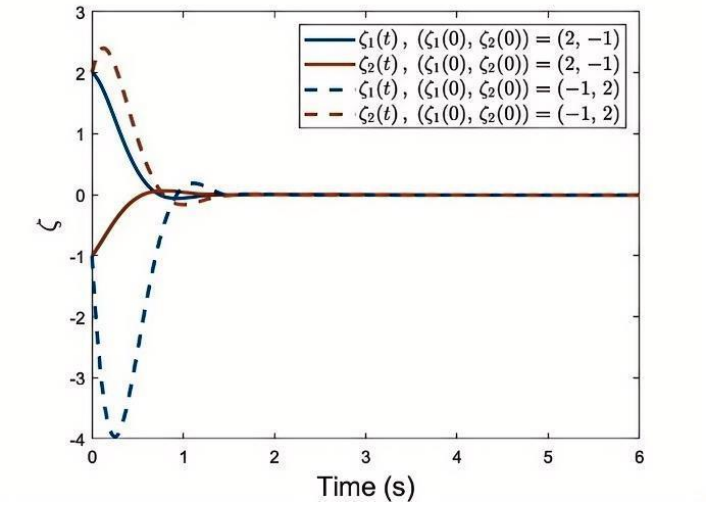

Figure 2. Responses of system (53) under controller (56) with different initial conditions ($T_p = 1.5$).

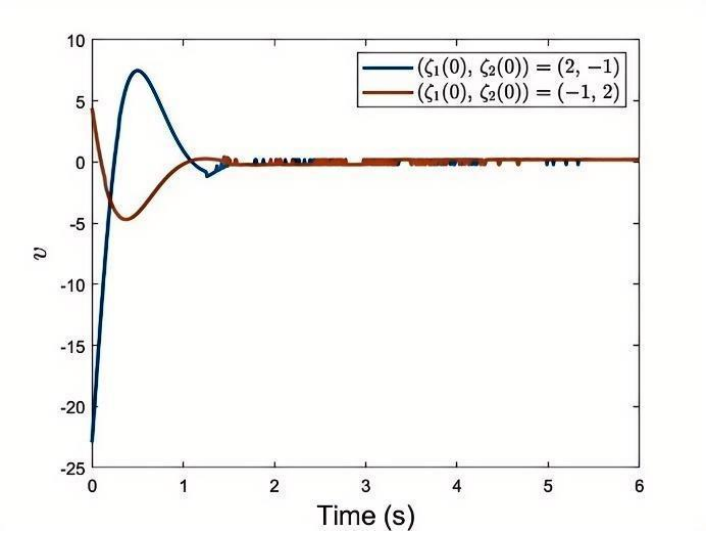

Figure 3. Responses of v ($T_p = 1.5$).

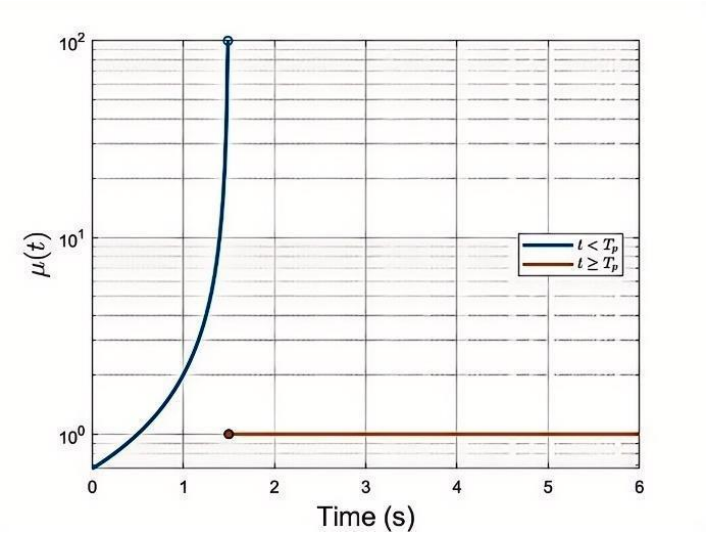

Figure 4. Responses of $\mu(t)$ ($T_p = 1.5$).

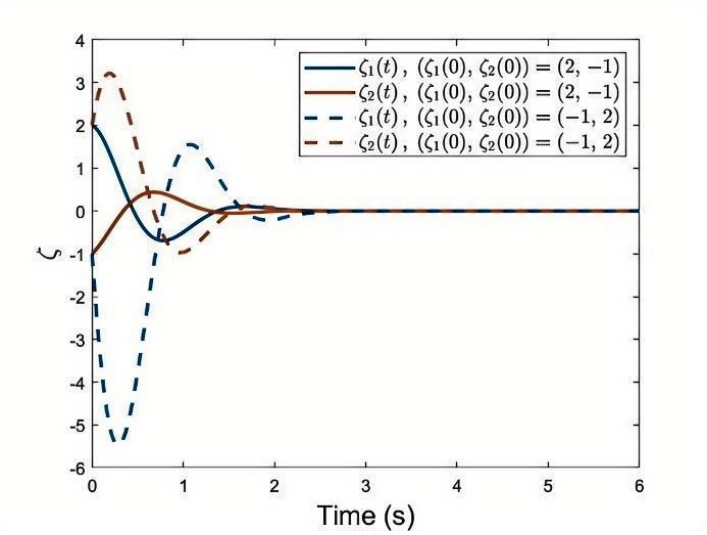

Figure 5. Responses of system (53) ($T_p = 3$).

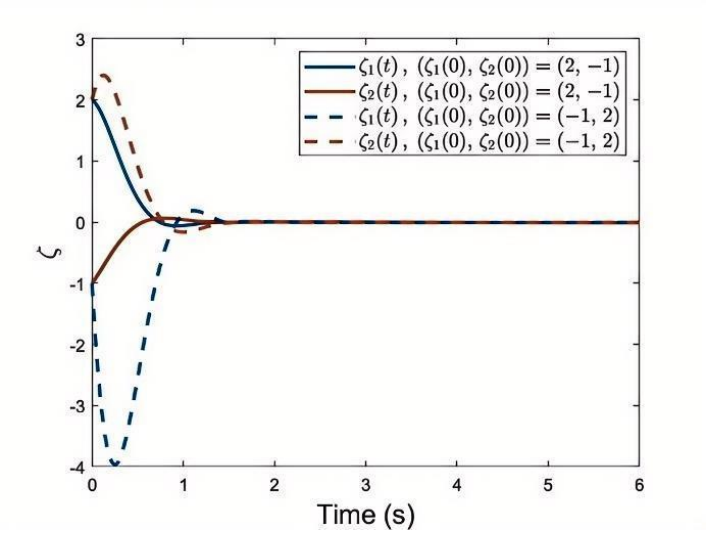

Figure 6. Responses of system (53) ($tanh(\,s/0.1), T_p = 1.5$).

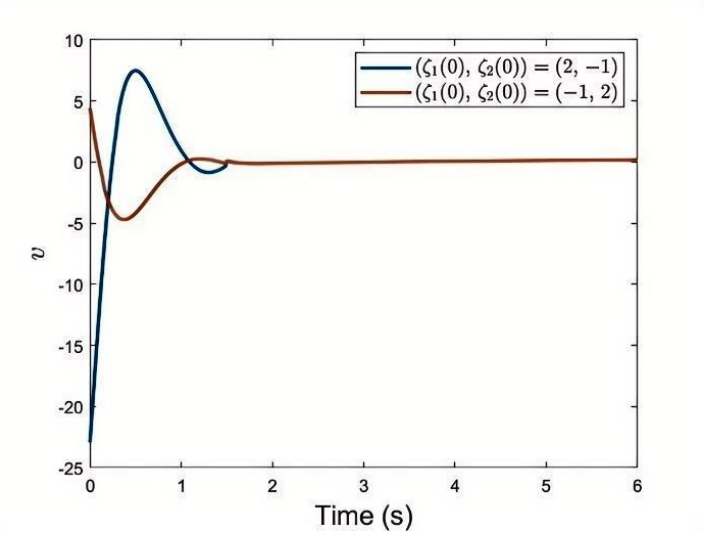

Figure 7. Responses of v $(tanh(s/0.1), T_p = 1.5)$.

From Figure 2, it can be seen that system (53) under controller (54) converges to 0 within $T_p = 1.5$ for different initial conditions and remains stable thereafter. Then it can be seen from Figure 3 that discontinuities arise from the introduction of the sign function in controller (56). From Figure 4, we can see the time profile of $\mu(t)$ (log scale) with $T_p = 1.5$: $\mu(t) = \frac{1}{T_p - t}$ for $0 \leq t < T_p$, and $\mu(t) = 1$ for $t \geq T_p$ (for practical implementation, T_p was advanced by 0.01 s).

To verify effectiveness, we further set $T_p = 3$. For the same initial conditions and controller parameters mentioned above, it can be seen from Figure 5 that system (53) converge to 0 within $T_p = 3$ and remains there thereafter, demonstrating prescribed-time performance.

To avoid discontinuity, the discontinuous $sign(s)$ can be replaced by $tanh(s/0.1)$ at $T_p = 1.5$. From Figures 6 and 7, under this case, system (53) exhibits satisfactory convergence performance under different initial conditions (practical prescribed-time stability), while the control input $v(t)$ remains continuous with significantly reduced chattering.

In summary, the feasibility of the control algorithm in Section 3.1 is demonstrated.

Example 2. Consider the system in [20] subject to external disturbances:

$$\begin{cases} \dot{\zeta}_1(t) = \zeta_2(t) + \theta\zeta_1(t), \\ \dot{\zeta}_2(t) = \zeta_3(t), \\ \dot{\zeta}_3(t) = v(t) + \theta\zeta_3^2(t) + 2\,sin(t), \end{cases} \tag{56}$$

where $\zeta_i(t) \in R, i = 1,2,3$, and θ is an uncertain parameter. Then $|2\,sin(t)| \leq \lambda = 2$. Take $T_p = 4$ (chosen by task requirements) and two initial conditions $(\zeta_1(0), \zeta_2(0), \zeta_3(0)) = (1, -1, -1), (-1,1, -1)$.

Under the strategy of [20], then from Figure 8, system (56) cannot be stabilized on $[T_p, +\infty)$. Hence, it is necessary to employ a new strategy, such as our strategy here.

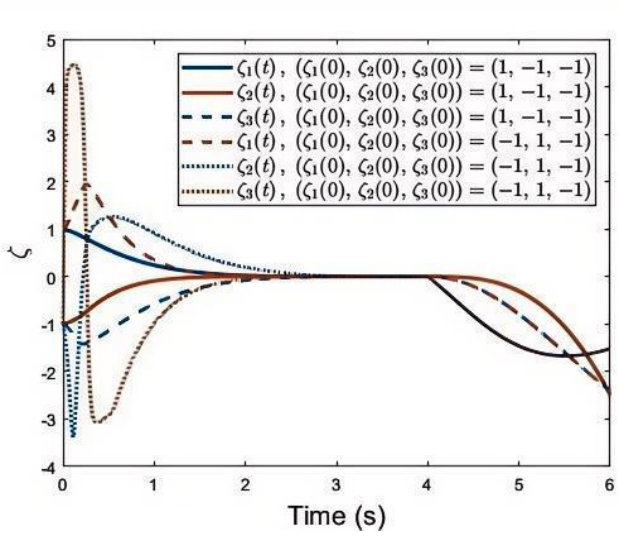

Figure 8. Responses of system (56) under the strategy of [20] with different initial conditions.

According to the control algorithm proposed above, the relevant controller and adaptive law are designed as

$$\dot{\hat{\theta}} = \begin{cases} \tau_s, t \in [0, T_p), \\ \tau_{s1} - g_m \mu \hat{\theta}, t \in [T_p, +\infty), \end{cases} \tag{57}$$

$$v(t) = \begin{cases} -g_3 \mu(t) s - \hat{\theta} \zeta_3^2 - 2\, sgn(s) + \varpi, t \in [0, T_p), \\ -g_3 s - \hat{\theta} \zeta_3^2 - 2\, sgn(s) + \varpi_1, t \in [T_p, +\infty), \end{cases} \tag{58}$$

$$\mu(t) = \begin{cases} \frac{1}{T_p - t}, t \in [0, T_p), \\ 1, t \in [T_p, +\infty), \end{cases} \tag{59}$$

where $\varpi = \frac{\partial \beta_2}{\partial \hat{\theta}} \dot{\hat{\theta}} + \frac{\partial \beta_2}{\partial t} + \frac{\partial \beta_2}{\partial \zeta_1}(\zeta_2 + \hat{\theta}\zeta_1) + \frac{\partial \beta_2}{\partial \zeta_2}\zeta_3 - \frac{1}{\mu}(w_3 + \beta_2 - \frac{\partial \beta_1}{\partial \hat{\theta}} \dot{\hat{\theta}} - \frac{\partial \beta_2}{\partial t} - \frac{\partial \beta_1}{\partial \zeta_1}(\zeta_2 + \hat{\theta}\zeta_1)) + (\zeta_3^2 - \frac{1}{\mu}\frac{\partial \beta_1}{\partial \zeta_1}\zeta_1)\frac{\partial \beta_2}{\partial \hat{\theta}} w_2 - \frac{1}{s} g_m \mu \hat{\theta}(\frac{\partial \beta_2}{\partial \hat{\theta}} w_3 + \frac{\partial \beta_1}{\partial \hat{\theta}} w_2)$, $\beta_1 = -g_1 \mu w_1 - \hat{\theta}\zeta_1$, $\beta_2 = -c_2 \mu w_2 - w_1 - \frac{\partial \beta_1}{\partial \hat{\theta}}\tau_2 + \frac{\partial \beta_1}{\partial \zeta_1}(\zeta_2 + \hat{\theta}\zeta_1) + \frac{\partial \beta_1}{\partial t}$, $s = w_3 + \frac{1}{\mu} w_2, t \in [0,4)$, $s = w_3 + w_2, t \in [4, +\infty)$, $\varpi_1 = \frac{\partial \beta_2}{\partial \hat{\theta}} \dot{\hat{\theta}} + \frac{\partial \beta_2}{\partial t} + \frac{\partial \beta_2}{\partial \zeta_1}(\zeta_2 + \hat{\theta}\zeta_1) + \frac{\partial \beta_2}{\partial \zeta_2}\zeta_3 - (w_3 + \beta_2 - \frac{\partial \beta_1}{\partial \hat{\theta}} \dot{\hat{\theta}} - \frac{\partial \beta_1}{\partial \zeta_1}(\zeta_2 + \hat{\theta}\zeta_1) + (\zeta_3^2 - \frac{\partial \beta_1}{\partial \zeta_1}\zeta_1)\frac{\partial \beta_2}{\partial \hat{\theta}} w_2$, $\tau_s = w_1 \zeta_1 - w_2 \frac{\partial \beta_1}{\partial \zeta_1}\zeta_1 + s\left(\zeta_3^2 - \frac{\partial \beta_2}{\partial \zeta_1}\zeta_1 - \frac{1}{\mu}\frac{\partial \beta_1}{\partial \zeta_1}\zeta_1\right)$, $t \in [0,4)$, $\tau_{s1} = w_1 \zeta_1 - w_2 \frac{\partial \beta_1}{\partial \zeta_1}\zeta_1 + s(\zeta_3^2 - \frac{\partial \beta_2}{\partial \zeta_1}\zeta_1 - \frac{\partial \beta_1}{\partial \zeta_1}\zeta_1), t \in [4, +\infty)$. Let $g_1 = g_2 = g_3 = 4, g_m = 0.4$, and the uncertain parameter be $\theta = 0.5$. The simulation results are shown in Figures 9 to 12.

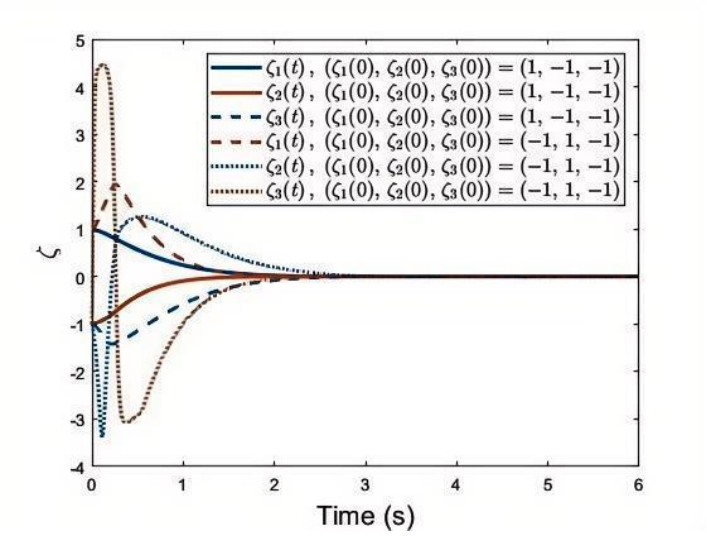

Figure 9. Responses of system (56) under controllers (57) and (58) with different initial conditions ($T_p = 4$).

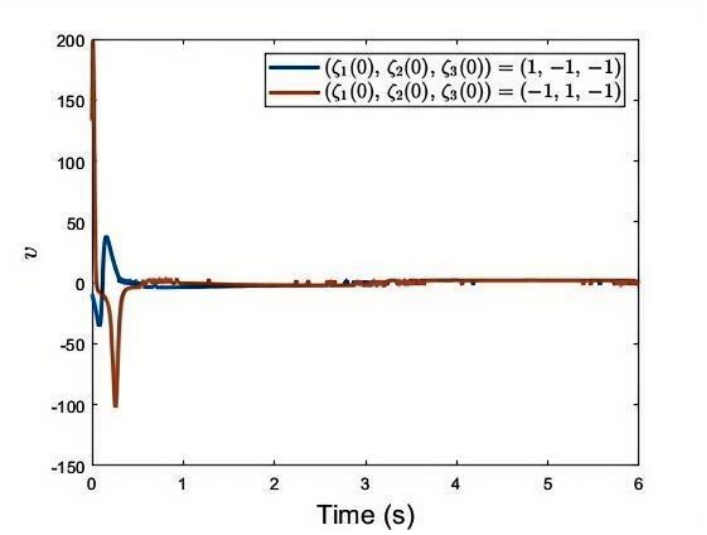

Figure 10. Responses of v ($T_p = 4$).

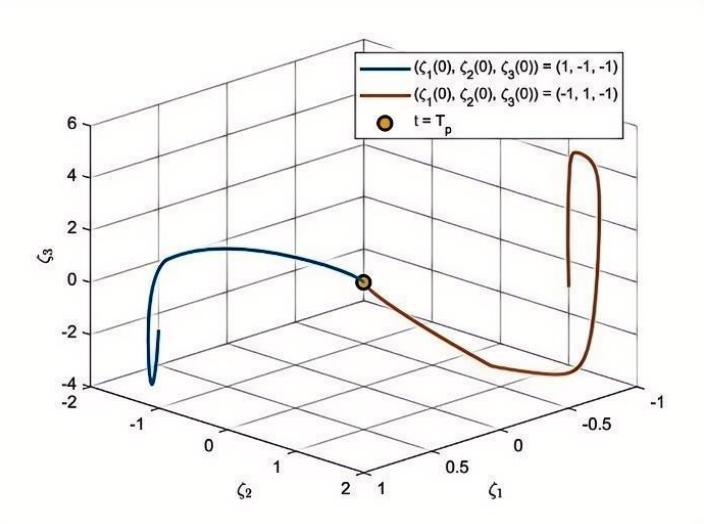

Figure 11. Responses of system (56) (3D, $T_p = 4$).

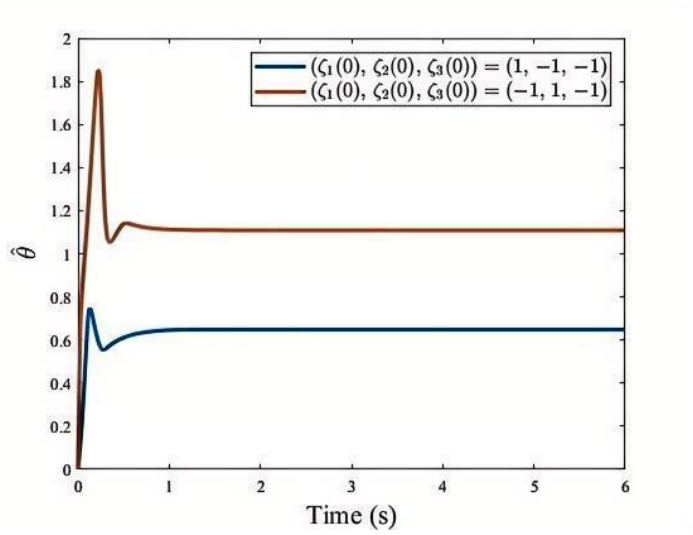

Figure 12. Responses of $\hat{\theta}$ ($T_p = 4$).

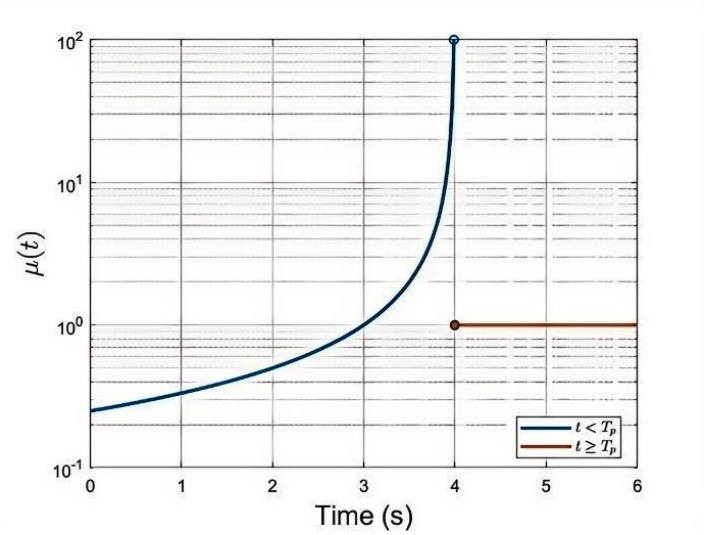

Figure 13. Responses of $\mu(t)$ ($T_p = 4$).

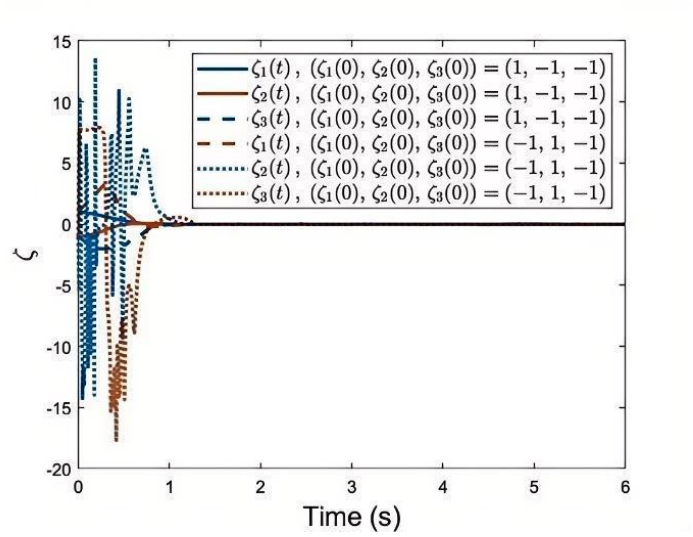

Figure 14. Responses of system (56) under controllers (57) and (58) with different initial conditions ($T_p = 1.3$).

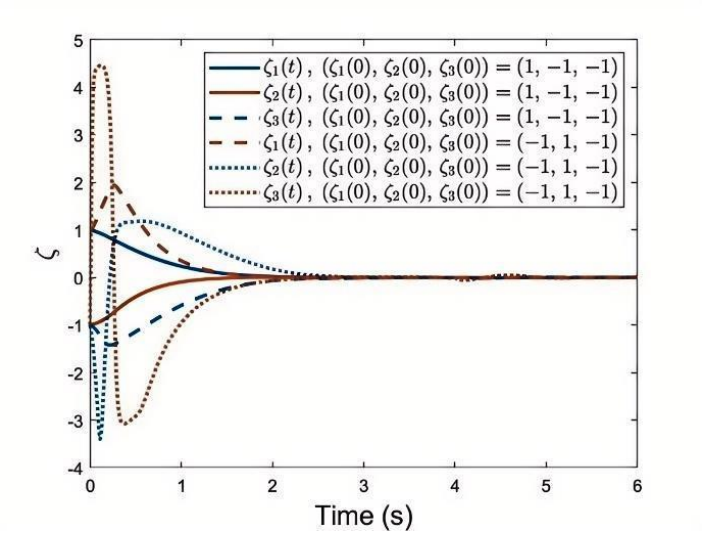

Figure 15. Responses of system (56) ($tanh(s/0.1), T_p = 4$).

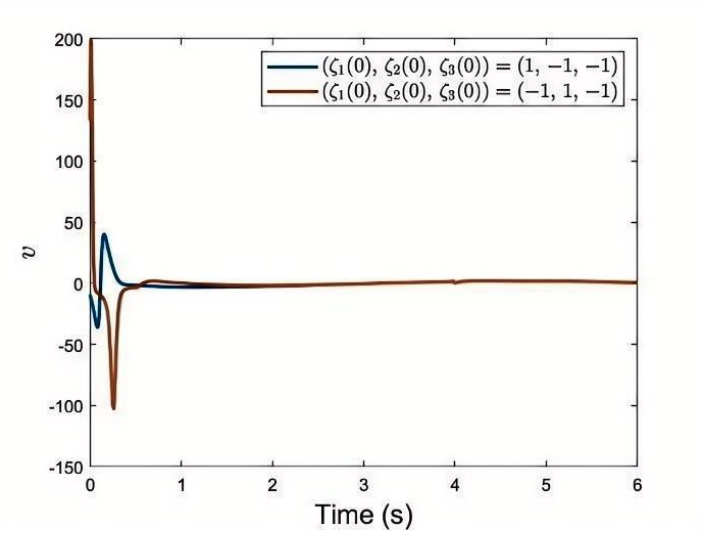

Figure 16. Responses of system (56) ($tanh(s/0.1), T_p = 4$).

From Figure 9, it can be seen that system (56) under controllers (57) and (58) converges to 0 within $T_p = 4$ for different initial conditions and also remain stable thereafter. Due to the introduction of the sign function, the controller reveals discontinuities as shown in Figure 10. Figure 11 shows the 3D trajectories of system (56). Figure 12 shows the trajectories of $\hat{\theta}$, which are bounded. From Figure 13, it can be seen that Time profile of $\mu(t)$(log scale) with $T_p = 4$: $\mu(t) = \frac{1}{T_p - t}$ for $0 \leq t < T_p$, and $\mu(t) = 1$ for $t \geq T_p$ (for practical implementation, T_p was advanced by 0.01 s).

To verify effectiveness, we further set $T_p = 1.3$. For the same initial conditions and controller parameters mentioned above, it can be seen from Figure 14 that $\zeta(t)$ converges to 0 within $T_p = 3$ and remains there thereafter, demonstrating prescribed-time performance.

To avoid discontinuity, the discontinuous $sign(s)$ is replaced with $tanh(s/0.1)$ at $T_p = 4$;

Figures 15 and 16 show that $\zeta(t)$ exhibits satisfactory convergence performance under different initial conditions (practical prescribed-time stability), while the control input $v(t)$ remains continuous with significantly reduced chattering.

In summary, the feasibility of the control algorithm in Section 3.2 is demonstrated.

5. Conclusions

This paper addressed prescribed-time control for nonlinear strict-feedback systems under external disturbances. For known nonlinearities, a backstepping controller with a first-order sliding layer at the last recursion achieved prescribed-time regulation while rejecting bounded disturbances; for unknown nonlinearities, an adaptive update embedded in the same structure let adaptation and robustness act together to drive the state to zero at a designer-chosen time under bounded disturbances. The settling time equaled the prescribed time, was independent of initial conditions and controller parameters, and could be fixed a priori by the task. From an engineering standpoint, the practical background covered here was limited and hardware validation was not yet included. As a concrete next step, we will extend the framework to stochastic nonlinear systems with process and measurement noise, use stochastic-stability reasoning with conservative regularization in the adaptive law to keep estimates bounded, incorporate implementation constraints (sampling, sensor noise, actuator limits), and evaluate the method on a lab platform to strengthen engineering applicability.

Author contributions

Litong Zhou: Investigation, Methodology, Writing—original draft, Validation; Lichao Feng: Conceptualization, Investigation, Supervision, Funding acquisition; Nan Ji: Investigation; Ruicheng Zhang: Validation, Software. All authors have read and approved the final version of the manuscript for publication.

Use of Generative-AI tools declaration

The authors declare they have not used Artificial Intelligence (AI) tools in the creation of this article.

Acknowledgments

This project is jointly supported by the Humanities and Social Science Fund of the Ministry of Education of China (23YJAZH031), Natural Science Foundation of Hebei Province of China (A2023209002), Tangshan Science and Technology Bureau Program of Hebei Province of China (24130201C), Fundamental Research Funds for Hebei Province Universities: North China University of Science and Technology (No. JJC2024045), and Graduate Student Innovation Fund of North China University of Science and Technology (2025S01).

Conflict of interest

The authors declare no conflicts of interest in this paper.

References

1. H. K. Khalil, *Nonlinear systems*, New Jersey: Prentice Hall, 2002.
2. J. Song, Y. Niu, Y. Zou, Finite-time stabilization via sliding mode control, *IEEE T. Automat. Contr.*, **62** (2017), 1478–1483. https://doi.org/10.1109/TAC.2016.2578300
3. W. Wang, C. Wen, Adaptive actuator failure compensation control of uncertain nonlinear systems with guaranteed transient performance, *Automatica*, **46** (2010), 2082–2091. https://doi.org/10.1016/j.automatica.2010.09.006
4. Z. Vukic, *Nonlinear control systems*, CRC Press, 2003. https://doi.org/10.1201/9780203912652
5. W. M. Haddad, A. L'Afflitto, Finite-time stabilization and optimal feedback control, *IEEE T. Automat. Contr.*, **61** (2016), 1069–1074. https://doi.org/10.1109/TAC.2015.2454891
6. S. P. Bhat, D. S. Bernstein, Lyapunov analysis of finite-time differential equations, In: *Proceedings of 1995 American Control Conference-ACC'95*, 1995, 1831–1832. https://doi.org/10.1109/ACC.1995.531201
7. S. P. Bhat, D. S. Bernstein, Finite-time stability of continuous autonomous systems, *SIAM J. Control Optim.*, **38** (2000), 751–766. https://doi.org/10.1137/S0363012997321358
8. Y. Hong, Y. Xu, J. Huang, Finite-time control for robot manipulators, *Syst. Control Lett.*, **46** (2002), 243–253. https://doi.org/10.1016/S0167-6911(02)00130-5
9. A. Polyakov, Nonlinear feedback design for fixed-time stabilization of linear control systems, *IEEE T. Automat. Contr.*, **57** (2012), 2106–2110. https://doi.org/10.1109/TAC.2011.2179869
10. H. Yang, D. Ye, Fixed-time stabilization of uncertain strict-feedback nonlinear systems via a bi-limit-like strategy, *Int. J. Robust Nonlin.*, **28** (2018), 5531–5544. https://doi.org/10.1002/rnc.4328
11. D. Gómez-Gutiérrez, On the design of nonautonomous fixed-time controllers with a predefined upper bound of the settling time, *Int. J. Robust Nonlin.*, **30** (2020), 3871–3885. https://doi.org/10.1002/rnc.4976
12. R. Aldana-López, D. Gómez-Gutiérrez, E. Jiménez-Rodríguez, J. D. Sánchez-Torres, A. G. Loukianov, On predefined-time consensus protocols for dynamic networks, *J. Franklin I.*, **357** (2020), 11880–11899. https://doi.org/10.1016/J.JFRANKLIN.2019.11.058
13. Y. Song, Y. Wang, J. Holloway, M. Krstic, Time-varying feedback for regulation of normal-form nonlinear systems in prescribed finite time, *Automatica*, **83** (2017), 243–251. https://doi.org/10.1016/j.automatica.2017.06.008
14. J. Holloway, M. Krstic, Prescribed-time observers for linear systems in observer canonical form, *IEEE T. Automat. Contr.*, **64** (2019), 3905–3912. https://doi.org/10.1109/TAC.2018.2890751
15. Z. Liu, C. Lin, Y. Shang, Prescribed-time adaptive neural feedback control for a class of nonlinear systems, *Neurocomputing*, **511** (2022), 155–162. https://doi.org/10.1016/j.neucom.2022.09.072

16. Y. Xiao, X. Xu, S. Dubljevic, Prescribed-time constrained tracking control of a class of 2×2 hyperbolic PDE systems with actuator dynamics, *Int. J. Robust Nonlin.*, **34** (2024), 6118–6141. https://doi.org/10.1002/rnc.7311
17. W. Li, M. Krstic, Stochastic nonlinear prescribed-time stabilization and inverse optimality, *IEEE T. Automat. Contr.*, **67** (2022), 1179–1193. https://doi.org/10.1109/TAC.2021.3061646
18. B. Zhou, Y. Shi, Prescribed-time stabilization of a class of nonlinear systems by linear time-varying feedback, *IEEE T. Automat. Contr.*, **66** (2021), 6123–6130. https://doi.org/10.1109/TAC.2021.3061645
19. P. Ning, C. Hua, K. Li, R. Meng, Event-triggered control for nonlinear uncertain systems via a prescribed-time approach, *IEEE T. Automat. Contr.*, **68** (2023), 6975–6981. https://doi.org/10.1109/TAC.2023.3243863
20. C. Hua, P. Ning, K. Li, Adaptive prescribed-time control for a class of uncertain nonlinear systems, *IEEE T. Automat. Contr.*, **67** (2022), 6159–6166. https://doi.org/10.1109/TAC.2021.3130883
21. J. J. E. Slotine, W. Li, *Applied nonlinear control*, Englewood Cliffs: Prentice Hall, 1991.
22. I. S. Khalil, J. C. Doyle, K. Glover, *Robust and optimal control*, Prentice Hall, 1995.
23. V. I. Utkin, *Sliding modes in control and optimization*, Berlin: Springer, 2013. https://doi.org/10.1007/978-3-642-84379-2
24. Z. Chen, X. Ju, Z. Wang, Q. Li, The prescribed time sliding mode control for attitude tracking of spacecraft, *Asian J. Control*, **24** (2022), 1650–1662. https://doi.org/10.1002/asjc.2569
25. H. Shen, J. Iorio, N. Li, Sliding mode control in backstepping framework for a class of nonlinear systems, *J. Mar. Sci. Eng.*, **7** (2019), 452. https://doi.org/10.3390/jmse7120452
26. S. Ullah, Q. Khan, A. Mehmood, A. I. Bhatti, Robust backstepping sliding mode control design for a class of underactuated electro-mechanical nonlinear systems, *J. Electr. Eng. Technol.*, **15** (2020), 1821–1828. https://doi.org/10.1007/s42835-020-00436-3
27. S. Ullah, Q. Khan, A. Mehmood, R. Akmeliawati, Integral backstepping integral sliding mode control of underactuated nonlinear electromechanical systems, *Control Eng. Appl. Inf.*, **21** (2019), 42–50.
28. E. Ahmad, A. Khan, S. Ullah, I. Youn, Pitch and yaw moment control of self-balancing two-wheeled electric vehicle via backstepping, In: *Proceedings of the 13th International Symposium on Mechanics, Aerospace and Informatics Engineering 2018*, 2018.
29. G. Bartolini, A. Ferrara, L. Giacomini, E. Usai, A combined backstepping/second-order sliding mode approach to control a class of nonlinear systems, In: *Proceedings. 1996 IEEE International Workshop on Variable Structure Systems. -VSS'96-*, 1996, 205–210. https://doi.org/10.1109/VSS.1996.578620
30. G. Bartolini, A. Ferrara, L. Giacomini, A. Usai, Properties of a combined adaptive/second-order sliding mode control algorithm for some classes of uncertain nonlinear systems, *IEEE T. Automat. Contr.*, **45** (2000), 1334–1341. https://doi.org/10.1109/9.867041
31. M. Defoort, A. Polyakov, G. Demesure, M. Djemai, K. Veluvolu, Leader-follower fixed-time consensus for multi-agent systems with unknown non-linear inherent dynamics, *IET Control Theory A.*, **9** (2015), 2165–2170. https://doi.org/10.1049/iet-cta.2014.1301

32. R. Aldana-López, D. Gómez-Gutiérrez, E. Jiménez-Rodríguez, J. D. Sánchez-Torres, M. Defoort, Enhancing the settling time estimation of a class of fixed-time stable systems, *Int. J. Robust Nonlin.*, **29** (2019), 4135–4148. https://doi.org/10.1002/rnc.4600
33. J. D. Sánchez-Torres, D. Gómez-Gutiérrez, E. López, A. G. Loukianov, A class of predefined-time stable dynamical systems, *IMA J. Math. Control I.*, **35** (2018), i1–i29. https://doi.org/10.1093/imamci/dnx004
34. E. Jiménez-Rodríguez, A. J. Muñoz-Vázquez, J. D. Sánchez-Torres, M. Defoort, A. G. Loukianov, A Lyapunov-like characterization of predefined-time stability, *IEEE T. Automat. Contr.*, **65** (2020), 4922–4927. https://doi.org/10.1109/TAC.2020.2967555
35. A. J. Muñoz-Vázquez, J. D. Sánchez-Torres, Predefined-time control of cooperative manipulators, *Int. J. Robust Nonlin.*, **30** (2020), 7295–7306. https://doi.org/10.1002/rnc.5171
36. R. Aldana-López, D. Gómez-Gutiérrez, E. Jiménez-Rodríguez, J. D. Sánchez-Torres, Generating new classes of fixed-time stable systems with predefined upper bound for the settling time, *Int. J. Control*, **95** (2022), 2802–2814. https://doi.org/10.1080/00207179.2021.1936190
37. S. V. Drakunov, D. B. Izosimov, A. G. Luk'yanov, V. A. Utkin, V. I. Utkin, The block control principle. I, *Avtomatika i Telemekhanika*, **5** (1990), 38–47.
38. A. G. Luk'yanov, Method of reducing equations for dynamics systems to a regular form, *Automat. Rem. Contr.*, **43** (1981), 413–420.
39. V. I. Utkin, S. V. Drakunov, D. E. Izosimov, A. G. Lukyanov, V. A. Utkin, A hierarchical principle of the control system decomposition based on motion separation, *IFAC Proc. Vol.*, **17** (1984), 1553–1558. https://doi.org/10.1016/S1474-6670(17)61197-2
40. Y. Song, H. Ye, F. L. Lewis, Prescribed-time control and its latest developments, *IEEE T. Syst. Man Cy. Syst.*, **53** (2023), 4102–4116. https://doi.org/10.1109/TSMC.2023.3240751
41. R. Seeber, Generalized Filippov solutions for systems with prescribed-time convergence, *Automatica*, **157** (2023), 111249. https://doi.org/10.1016/j.automatica.2023.111249
42. R. Aldana-López, D. Gómez-Gutiérrez, E. Jiménez-Rodríguez, J. D. Sánchez-Torres, M. Defoort, Enhancing the settling time estimation of a class of fixed-time stable systems, *Int. J. Robust Nonlin.*, **29** (2019), 4135–4148. https://doi.org/10.1002/rnc.4600
43. L. Feng, C. Zhang, M. Abdel-Aty, J. Cao, F. E. Alsaadi, Prescribed-time trajectory tracking control for a class of nonlinear system, *Electron. Res. Arch.*, **32** (2024), 6535–6552. https://doi.org/10.3934/era.2024305
44. R. Aldana-López, R. Seeber, D. Gómez-Gutiérrez, M. T. Angulo, M. Defoort, A redesign methodology generating predefined-time differentiators with bounded time-varying gains, *Int. J. Robust Nonlin.*, **33** (2023), 9050–9065. https://doi.org/10.1002/rnc.6315
45. D. Gómez-Gutiérrez, R. Aldana-López, R. Seeber, M. T. Angulo, L. Fridman, An arbitrary-order exact differentiator with predefined convergence time bound for signals with exponential growth bound, *Automatica*, **153** (2023), 110995. https://doi.org/10.1016/j.automatica.2023.110995
46. R. Aldana-López, R. Seeber, H. Haimovich, D. Gomez-Gutierrez, On inherent limitations in robustness and performance for a class of prescribed-time algorithms, *Automatica*, **158** (2023), 111284. https://doi.org/10.1016/j.automatica.2023.111284
47. V. Parra-Vega, Second order sliding mode control for robot arms with time base generators for finite-time tracking, *Dyn. Control*, **11** (2001), 175–186. https://doi.org/10.1023/A:1012535929651

48. V. Parra-Vega, G. Hirzinger, TBG sliding surfaces for perfect tracking of robot manipulators, In: *Advances in variable structure systems: Analysis, integration and applications*, 2000, 115–124. https://doi.org/10.1142/9789812792082_0010
49. T. Tsuji, P. G. Morasso, M. Kaneko, Feedback control of nonholonomic mobile robots using time base generator, In: *Proceedings of 1995 IEEE International Conference on Robotics and Automation, Nagoya, Japan, 1995*, 1995, 1385–1390. https://doi.org/10.1109/ROBOT.1995.525471
50. T. Sun, L. Cheng, Z. Hou, M. Tan, Novel sliding-mode disturbance observer-based tracking control with applications to robot manipulators, *Sci. China Inf. Sci.*, **64** (2021), 172205. https://doi.org/10.1007/s11432-020-3043-y

AIMS Press